RUSSIAN JOURNAL OF ELECTROCHEMISTRY, 2025, Vol. 61, No. 1, pp. 37–51

ALL SOLID STATE THIN-FILM LITHIUM-ION BATTERIES (REVIEW)[1]

© 2025 A. M. Skundin*, T. L. Kulova

Frumkin Institute of Physical Chemistry and Electrochemistry, Russian Academy of Sciences, Moscow, Russia

**e-mail: askundin@mail.ru*

Received: June 25, 2024

Revised: September 05, 2024

Accepted: September 25, 2024

Abstract. The main features of all-solid-state lithium-ion batteries and similar batteries with a lithium metal electrode are considered. The main areas of application of such batteries are noted. Solid inorganic electrolytes and electrode materials are considered in detail. The main manufacturers are briefly listed.

Keywords: *li-ion battery, lithium electrode, solid electrolyte, electrode materials*

DOI: 10.31857/S04248570250102e3

INTRODUCTION

All-solid-state thin-film lithium-ion batteries [1] represent a special, relatively small, but very important category of such devices. All-solid-state batteries have certain advantages over traditional batteries with liquid electrolytes. Firstly, the absence of organic solvents increases the safety of the battery by eliminating the risk of possible leakage of liquid and vapors and, consequently, reducing the risk of fire and explosion. Secondly, liquid electrolyte solvents are often involved in the degradation of lithium-ion batteries, so it is assumed that the service life of solid-state batteries will be much longer. Thirdly, the use of liquid electrolyte leads to a number of limitations on the design and size of the battery. (The typical thickness of conventional separators in lithium-ion batteries is about 20 μm, while the thickness of solid electrolytes is 1 μm). Thus, the concept of all-solid-state devices opens the way to the creation of thin-film (including flexible and transparent) and microbatteries.

The need for all-solid-state thin-film lithium-ion batteries arises due to the rapidly developing microelectronics, especially with the advent of battery-powered smart cards, radio frequency identification (RFID) tags, smart watches, implantable medical devices, remote micro sensors and transmitters, Internet of Things (IoT) systems and various other wireless devices, including intelligent building management and so on. Often, these batteries need to be placed on the same chip as the microelectronics device itself, creating a so-called embedded system. The manufacturing technology of solid-state thin-film lithium-ion batteries must be compatible with the manufacturing technology of integrated circuits, microelectromechanical systems (MEMS devices), semiconductor sensors, etc., i.e., in general, it must be VLSI-compatible (VLSI: "very large scale integration"). Flexible and transparent devices are quite important types of thin-film batteries. It should be noted that significant progress in the field of solid-state lithium-ion batteries has recently been achieved through the experimental development and optimization of solid electrolytes and functional electrode materials.

Interest in all-solid-state lithium-ion batteries is steadily increasing. The number of publications on this topic in 2010 was about 500, and in 2021 it exceeded 2,500 [2]. Fairly detailed review papers can be mentioned [3–16].

GENERAL PROVISIONS

A schematic diagram of an all-solid-state thin-film lithium-ion battery is shown in Fig. 1.

The negligible thickness of a thin-film battery forces it to be placed on a more or less large structural element (substrate), which may be part of a device powered by this battery. And this is perhaps the main difference between thin-film batteries and conventional commercial lithium-ion batteries. The second fundamental difference is the possibility of using lithium metal as a negative electrode in all-solid-state batteries. It is known that the main feature of lithium-ion batteries is the use of intercalation electrodes instead of lithium metal.

The structural base of a thin-film battery can in principle be made of any material, including metals, ceramics, glass, polymers, and even paper. If this material is an electronic conductor, then the structural

[1] Based on the materials of the report at the 17th International Meeting "Fundamental and applied problems of solid state ionics", Chernogolovka, June 16–23, 2024.

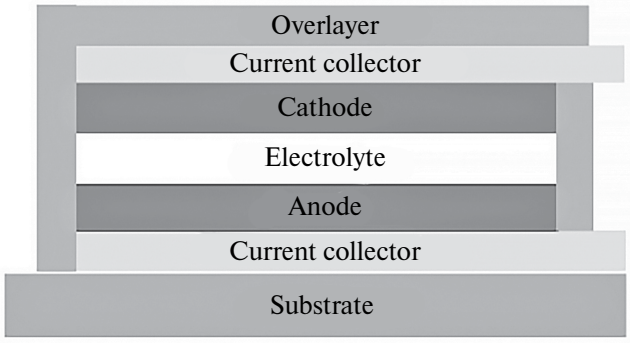

Fig. 1. Diagram of an all-solid-state thin-film lithium-ion battery.

base (substrate) can play the role of a current collector of one electrode (usually lithium). In any case, the substrate material must comply with the conditions of application and operation of the functional layers. The substrate material should not interact with other layers of the battery. The substrate material should also prevent lithium from diffusing from the battery. The battery, in fact, consists of two electrodes, between which there is an electrolyte. The outside of each electrode is in contact with the corresponding current collector. The battery as a whole is enclosed in an appropriate housing. The housing is a very important structural element. It must protect the internal contents of the battery from external physical and chemical influences, in particular, prevent the interaction of active battery materials with air and moisture. Ideally, the battery and the electronic device powered by it should be functionally integrated with maximum efficiency and voltage control.

Although the first attempts to create fully solid-state thin–film batteries were made back in the 1950s, real success was achieved only 40 years later and was due to the development of a successful solid electrolyte, LiPON – lithium phosphorus oxynitride [17–20] which is obtained by magnetron radiofrequency sputtering of a Li_3PO_4 target in a nitrogen medium. Its average composition can be expressed as $Li_{3.3}PO_{3.8}N_{0.22}$ with some uncertainty of nitrogen content. It was assumed that the introduction of nitrogen into the glass structure would increase its chemical and thermal stability. LiPON is stable in contact with lithium metal, has very low electronic conductivity and adequate ionic conductivity of about 2.3 μS/cm at room temperature, and most importantly, has a lithium transfer number equal to unity. The decomposition voltage of LiPON exceeds 5.5 V. Using this very electrolyte, thin-film batteries with various active materials of the positive electrode, including $Li_xMn_2O_4$, TiS_2, $LiCoO_2$ и V_2O_5, have been manufactured.

In the first decade of the 21st century, several companies launched the production of all-solid-state thin-film batteries with capacities from 0.1 to 5 mAh. These batteries used negative electrodes made of both lithium and conventional intercalation materials (Sn, Si, Ge, and C). Total thickness of the active part (current sinks, electrodes and electrolyte) ranged from 20 to 50 μm. The first LiPON electrolyte batteries could withstand hundreds and even thousands of cycles with low degradation. Such excellent cyclicity was explained by a combination of several factors. Firstly, the high stability of LiPON, secondly, the ability of thin-film materials to withstand volumetric changes caused by lithiation and delithiation, and thirdly, the uniform distribution of current in the thin-film structure.

The diagram in Fig. 1 shows a "plate-like" (one-dimensional) structure. Various 3D constructions are more rational [4, 21–27]. 3D designs can significantly increase the specific energy of the battery, as the total surface area of the electrodes per unit area of the substrate increases. In fact, the energy needs of micro- and nanoelectromechanical systems, including implantable medical devices, drug delivery systems, microsensors, etc., have opened up a niche for 3D batteries with a characteristic size from 1 to 10 mm^3 and a capacity from 10 nW to 1 mW.

Various designs of 3D batteries with regular or chaotic geometry are described. It can be a periodic grid or an aperiodic ensemble of electrodes. For example, it can be an array of cylindrical (columnar) electrodes of both signs grown on substrates. Two arrays of different electrodes are inserted into each other. The space between the electrodes must be filled with electrolyte (Fig. 2). The main disadvantages of this design are a rather large volume of electrolyte, a large and variable interelectrode distance.

A more effective design is one consisting of an array of column electrodes of the same sign placed on a substrate and coated with a thin layer of electrolyte. In this case, the remaining space is filled with the active material of the counter-electrode.

An interesting 3D battery design is described in [21]. Here, a number of grooves are made in a massive silicon substrate by anisotropic etching. The substrate itself plays the role of a single current collector. The active electrode layers are deposited inside this highly structured substrate, starting with an effective barrier layer, preferably TiN or TaN, to protect the substrate from lithium penetration, followed by a thin-film silicon negative electrode with a thickness of about 50 nm, a solid-state LiPON-like electrolyte and a thin-film material of the positive electrode, in this example $LiCoO_2$ with a thickness of 1 μm. The second current collector is applied last.

The chaotic analogue of the regular structure shown in Fig. 2 is a kind of "sponge" design (Fig. 3). In this case, the solid mesh of the sponge ("web"), which is the cathode, is covered with a very thin layer of solid electrolyte. The remaining voids are filled with anode material.

Probably the most advanced technology for the production of 3D batteries is 3D printing (in the English-language literature, additive manufacturing (AM)) [28–30]. This technology makes it possible to produce objects with well-controlled and very complex geometries through layer-by-layer deposition directly on computerized equipment without using any templates. Recently, 3D printing of lithium-ion batteries of various geometries has been developed in order to increase their specific energy, specific power and mechanical characteristics. In fact, 3D printing is not a single method, but a group of methods that includes: (i) material extrusion (for example, direct ink writing, DIW, and fused deposition modeling, FDM); (ii) inkjet processing of materials (for example, inkjet printing); (iii) binder jet cleaning; (iv) powder layer melting (e.g., selective laser sintering and selective laser melting); (v) directed energy release; (vi) photopolymerization (e.g., stereolithography (SLA)); (vii) sheet lamination. The most popular 3D printing method used in the manufacture of lithium-ion batteries is direct ink writing. The DIW equipment is not complicated (and therefore inexpensive) and includes a simple desktop 3D printer, a heated table, a pneumatic dispenser, and a micronozzle.

A kind of 3D version of an all-solid-state lithium-ion battery is a transparent (or translucent) flexible battery. The concept of a translucent battery with opaque active electrode materials was proposed in 2011 [31] and developed later [32]. The concept is based on the principle of electrodes with a mesh structure. A distinctive feature of this mesh design is the fact that the size of the electrodes is lower than the resolution of the human eye, and thus the entire battery appears transparent. [31] described a thin-film battery of the $LiMn_2O_4/Li_4Ti_5O_{12}$ electrochemical system with a gel polymer electrolyte, whereas [32] described a $LiCoO_2$/Si battery with LiPON electrolyte. The transparency of both batteries is close to 60%.

FUNCTIONAL MATERIALS FOR SOLID-STATE THIN-FILM LITHIUM–ION BATTERIES

Materials for electrolytes. The electrolytes of solid-state thin-film batteries are fundamentally different from those of traditional lithium-ion batteries, and quite a lot of research has been devoted to the development

Fig. 2. 3D design with interdigital arrays of electrodes.

and improvement of such electrolytes (see, for example, reviews [33–42]).

Electrolytes for solid-state thin-film batteries must have high ionic and low electronic conductivity at operating temperature (preferably room temperature), a wide electrochemical stability window, adaptability, and compatibility with electrodes. The latter feature suggests that the electrolyte must be resistant to interaction with electrodes, especially with lithium and lithium alloy electrodes, and have the same coefficients of thermal expansion with both electrodes. Both crystalline and amorphous materials are used as solid electrolytes. A typical representative of an amorphous (glass-like) electrolyte for solid-state thin-film batteries is the already mentioned LiPON. Other examples of amorphous solid electrolytes are oxide and sulfide glass. Crystalline solid electrolytes are represented by solid solutions with a perovskite structure, lithium-ion conductors such as NASICON, LISICON and thio-LISICON, as well as lithium-ion conductors of the garnet type.

An interesting example of a LiPON-like glassy electrolyte is the so-called LiSON with a typical composition of $Li_{0,29}S_{0,28}O_{0,35}N_{0,09}$ and an ionic conductivity of about 2×10^{-5} S/cm [43]. This material was produced by RF magnetron sputtering using a Li_2SO_4 target in an atmosphere of pure nitrogen. Another similar glassy electrolyte, known as LiPOS ($6LiI\text{-}4Li_3PO_4–P_2S_5$), has the same conductivity [44].

Sulfide glassy solid electrolytes, especially those with a high concentration of Li+ ions, have generally higher conductivity than LiPON-like electrolytes. In the $Li_2S–P_2S_5$ system, when the Li_2S content is more than 70 mol.%, the electrolytes have a conductivity of more than 10^{-4} S/cm, which is one and a half orders of magnitude higher than the conductivity of LiPON-like analogues. However, the synthesis of sulfide glass with a sufficiently high concentration of Li+ ions is difficult due to easy crystallization during cooling, so such glass is made by double-roll rapid quenching or mechanical milling. The addition of halides, borohydride, or lithium

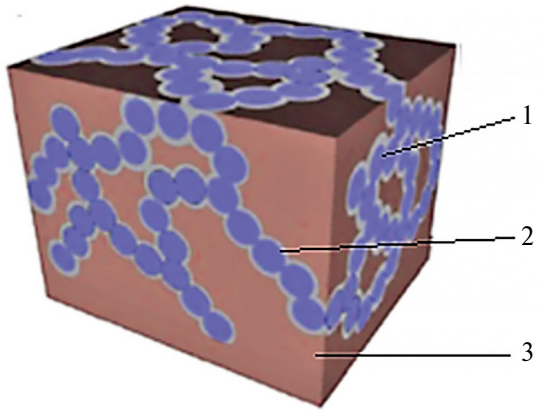

Fig. 3. The "spongy" design of the 3D battery. 1 is the active material of the positive electrode, 2 is the electrolyte, 3 is the active material of the negative electrode (from [24], open access).

orthophosphate increases the conductivity of the glass to 10^{-3} S/cm at room temperature. For example, an electrolyte of composition $95(80Li_2S\text{-}20P_2S_5) + 5LiI$ has a conductivity of 2.7 mS/cm [45], an electrolyte of composition $Li_{5.5}PS_{4.5}Cl_{1.5}$ with an argyrodite structure is 10.2 mS/cm [46], and an electrolyte of composition $Li_{5.4}PS_{4.4}Cl_{1.6}$ is 8.4 mS/cm [47].

Intermediate forms, the so-called glass-ceramic electrolytes, represent a kind of palliative. Their conductivity is higher than that of amorphous electrolytes, but lower than that of crystalline electrolytes. Such glass-ceramic electrolytes can be obtained by crystallization of real glass electrolytes. The separation of thermodynamically stable crystalline phases from the initial glass leads to a decrease in intercrystalline resistance. For example, glass–ceramic electrolytes obtained by heat treatment of $Li_2O–Al_2O_3–TiO_2–P_2O_5$ glasses are described in [48]. The maximum conductivity of 1.3 mS/cm was achieved in a system heat-treated at a temperature of 950 °C.

Glass ceramics of the compositions $70Li_2S–30P_2S_5$ [49], $80Li_2S\text{-}20P_2S_5$ [50], $Li_{3,25}P_{0,95}S_4$ [51] и $Li_7P_3S_{11}$ [51] have even higher conductivity. Glass ceramics $70Li_2S\text{-}30P_2S_5$ were synthesized by heat treatment of the corresponding glass at a temperature of about 240 °C (slightly higher than the crystallization temperature). This treatment resulted in an increase in conductivity at room temperature to 3.2 mS/cm. The conductivity of glass ceramics $80Li_2S\text{-}20P_2S_5$ is 0.74 ms/cm. Glass ceramics $Li_{3.25}P_{0.95}S_4$ and $Li_7P_3S_{11}$ demonstrate conductivity at room temperature of 1.3 and 17 mS/cm (!) The glass-ceramic electrolyte $Li_7P_3S_{11}$ ($70Li_2S\text{-}30P_2S_5$) is characterized not only by the highest conductivity, but also by the lowest activation energy of 17 kJ/mol at room temperature (and, consequently, the weakest temperature dependence of conductivity).

The most popular crystalline electrolytes of the (ABO_3) type peroxite family with A = Li, La, and B = Ti are solid solutions with the general formula $Li_{3x}La_{2/3\text{-}x\text{-}1/3–2x}TiO_3$ (where the square indicates the lattice vacancy) [52]. Usually $0.04<x<0.17$, in this case the abbreviation LLTO is used. Such electrolytes have a conductivity at room temperature of about 1 mS/cm. Lithium-enriched oxyhalides with an anti-perovskite structure have an even higher conductivity. For example, the compound $Li_3OCl_{0.5}Br_{0.5}$ exhibits a specific conductivity of about 2 mS/cm at room temperature and about 5 mS/cm at 230 °C [53].

A classic example of an electrolyte with the NASICON structure is $NaA^{IV}_2(PO_4)_3$, where A^{IV}=Ge, Ti, and Zr. Such a structure can be represented as a $[A_2P_3O_{12}]–$ framework consisting of AO_6 octahedra and PO_4 tetrahedra. The most popular Li^+ conducting electrolyte with a NASICON-like structure is $Li_{1.3}Al_{0.3}Ti_{1.7}(PO_4)_3$ (LATP), belonging to the family with the general formula $Li_{1+x}Ti_{2\text{-}x}M_x(PO_4)_3$ (M=Al, Ga, B, Sc). Among Li^+-conducting electrolytes with a NASICON-like structure, $Li_{1+x}Al_xGe_{2\text{-}x}(PO_4)_3$ (LAGP) has the highest conductivity at room temperature of 3 mS/cm^3. Of particular interest is a silicon-substituted electrolyte in which part of the phosphorus is replaced by silicon $Li_{1+x+y}Ti_{2\text{-}x}Al_xSi_y(PO_4)_{3\text{-}y}$.

The electrolyte analogue with the NASICON – LISICON structure with the formula $Li_{2+2x}Zn_{1\text{-}x}GeO_4$ has too low conductivity and is of no practical interest. At the same time, thio-LISICON is very attractive [54]. The highest conductivity, 2.2 mS/cm, is shown by an electrolyte of the composition $Li_{3.25}Ge_{0.25}P_{0.75}S_4$ (which can be considered as $Li_{4\text{-}x}Ge_{1\text{-}x}P_xS$ with x=0.75). At the same time, the $Li_2S–GeS_2–P_2S_5$ electrolytes proved to be incompatible with the graphite negative electrode. To solve this problem, the authors of [55] proposed a battery design with a two-layer solid electrolyte. The layer facing the negative (graphite) electrode is $LiI–Li_2S–P_2S_5$ glass, and the layer facing the positive ($LiCoO_2$) electrode is $Li_2S–GeS_2–P_2S_5$ crystalline material. It is known that the first electrolyte is resistant to electrochemical reduction, and the second to oxidation.

An even higher conductivity, 12 ms/cm, is provided by a similar superionic conductor of the composition $Li_{10}GeP_2S_{12}$ with a special crystal structure [56].

Special attention has recently been paid to solid electrolytes with structures similar to garnet. Ideal garnets can be represented by the general formula $A_3B_2(XO_4)_3$, where A = Ca, Mg, Y, La or rare earth elements; B = Al, Fe, Ga, Ge, Mn, Ni or V; X = Si, Ge or Al. The most important feature of the garnet

structure is the ability to introduce Li^+ ions into the structure. Garnets usually contain from five to seven Li atoms per formula unit. An increase in the number of lithium atoms in the formula unit to five, as, for example, in $Li_5La_3B'_2O_{12}$ (B' = Bi, Sb, Na, Ta), leads to an increase in ionic conductivity by three orders of magnitude to 2×10^{-5} S/cm [57]. Partial replacement of Zr in lithium-enriched garnet $Li_7La_3Zr_2O_{12}$ with Nb makes it possible to obtain a material with lithium-ion conductivity up to 0.8 mS/cm [58]. $Li_7La_3Zr_2O_{12}$ doped with Ga has an ionic conductivity of 0.54 mS/cm [59]. For substituted garnet $Li_{6.75}La_3Zr_{1.75}Ta_{0.25}O_{12}$, room temperature conductivity of 0.9 mS/cm was reported [60]. Doping of an electrolyte with a garnet structure by a bromide anion leads to a two-three-fold increase in the conductivity of Li^+ ions.

Fig. 4 summarizes the temperature dependence of the conductivity of various solid electrolytes. As a rule, these dependences are well described by the Arrhenius equation (unlike many liquid electrolytes). Fig. 4 also clearly shows how the conductivity of the new electrolytes has increased compared to LiPON.

Materials for negative electrodes. As already mentioned, a significant advantage of solid-state thin-film batteries is the possibility of using lithium metal as a negative electrode. Lithium has the maximum theoretical specific capacity and the most negative equilibrium potential, therefore, the use of lithium metal, all other things being equal, provides the highest discharge voltage. However, the use of lithium metal as a rechargeable negative electrode in batteries with liquid aprotic electrolyte encounters well-known fundamental problems of dendrite formation and encapsulation. Both problems lead to a drastic reduction in service life.

When lithium metal comes into contact with a solid electrolyte, the problems of dendrite formation do not play such a decisive role as in the case of liquid electrolytes. This statement is clearly confirmed by the successful commercialization of fully solid-state batteries with a lithium metal negative electrode, implemented at Oak Ridge National Laboratory (USA) at the beginning of the current millennium, as well as in companies such as STMicroelectronics, CymbetTM Corp., Front Edge Technology, Inc., Exxellatron, etc. For example, STMicroelectronics claimed that its thin-film batteries last up to 4,000 cycles. To combat dendrite formation at the interface with solid electrolytes, the same techniques are used that have been developed in systems with liquid electrolyte, primarily the creation of a lithium-ion current-carrying substrate and the application of artificial SEI (solid electrolyte interface, passive film) [61].

As a rule, lithium electrodes are applied by thermal evaporation or magnetron sputtering directly onto a solid electrolyte [62]. The typical thickness of a lithium thin–film electrode is 2–5 μm, which corresponds to a capacity of 0.4–1.0 mAh/cm^2.

A serious disadvantage of lithium metal negative electrode batteries is the limited operating temperature, determined by the melting point of lithium (180.54 °C). Since thin-film solid-state batteries are designed primarily for microelectronic devices, these batteries are used in modern semiconductor technology, i.e. they should be suitable for soldering at higher temperatures. A rather ingenious option to solve this problem is the so-called "lithium-free construction" [63]. Such a lithium-free battery is assembled without lithium metal (and, therefore, can withstand high-temperature solder melting procedures), but with some excess of the active material of the positive electrode. During the first charge, the required amount of lithium is deposited on the current collector. (In this respect, "lithium-free" batteries are similar to the recently popular so-called "anode-free" batteries.) For a lithium-free battery to function properly, it is very important that the negative electrode current collector material does not form intermetallic compounds with lithium. The most suitable material in this regard is copper, which is used as current receivers in conventional lithium-ion batteries, although some alternative materials such as Ti, Co and TiN are also being discussed.

Another approach to increase the operating temperature of thin-film solid-state batteries is to replace pure lithium with a lithium alloy, such as an alloy with magnesium. The melting point of such an alloy, depending on the magnesium content, ranges from 200 °C with a magnesium content of 4 at.% up to 400 °C with a magnesium content of 40 at.%.

However, a more fundamental solution to the problem is to replace the lithium electrode with an electrode typical of lithium-ion batteries, that is, an electrode in which lithium ions are reversibly embedded in a matrix. Elements of the 4th group of the Periodic Table (carbon, silicon, germanium, tin), oxides and some other compounds can be used as such matrices (as in traditional lithium-ion batteries).

Silicon is known to have a record capacity for the reversible incorporation of lithium. When lithium is introduced into silicon, intermetallic alloys are formed, and the most lithium-rich intermetallic compound is $Li_{4.4}Si$ ($Li_{22}Si_5$), which corresponds to a specific capacity of 4200 mAh/g. Such an alloy is formed only at elevated temperatures. At room temperature, the most lithium-rich intermetallic compound is $Li_{3.75}Si$ ($Li_{15}Si_4$), which corresponds to a specific capacity of 3590 mAh/g. It should be emphasized that these specific capacity values relate to the process of introducing lithium into silicon,

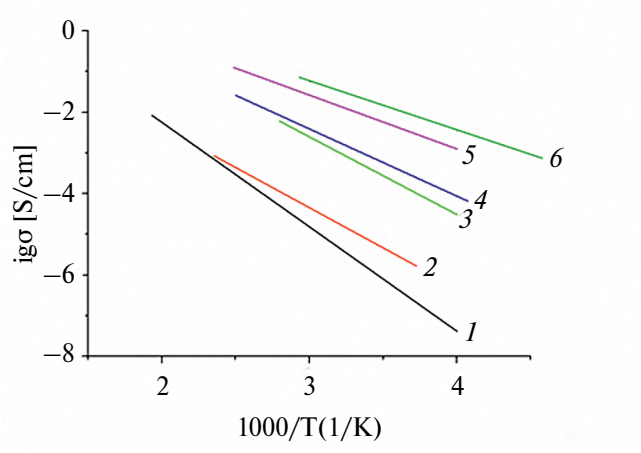

Fig. 4. Temperature dependence of the specific conductivity of solid electrolytes. *1* – LiPON, *2* – $Li_{3.6}Si_{0.6}P_{0.4}O_4$, *3* – $Li_{0.5}La_{0.5}TiO_3$, *4* – glass-ceramic $Li_7P_3S_{11}$, *5* – $Li_{10}GeP_2S_{12}$, *6* – $Li_{9.54}Si_{1.74}P_{1.44}S_{11.7}Cl_{0.3}$.

i.e. to the charge of the negative electrode. During discharge, i.e., when lithium is extracted from $Li_{3.75}Si$ intermetallide, the specific capacity is 1852 mAh/g (recall that the specific capacity of pure lithium is 3828 mAh/g). The introduction of lithium into silicon proceeds at potentials close to the potential of lithium, and its anode extraction is mainly in the range of 0.3–0.5 V (Li^+/Li).

The fundamental possibility of long-term operation of a silicon electrode in contact with a solid electrolyte (LiPON) was experimentally confirmed in [64]. In [65], a boron-doped LiPON electrolyte was used. In a later work [66], the compatibility of porous silicon with a glassy electrolyte of the composition $80Li_2S{\cdot}20P_2S_5$ was shown. In this work, for 100 cycles, the capacity of the silicon electrode was almost 3000 mAh/g. In [67, 68], the operability of amorphous silicon electrodes in contact with a glass-ceramic electrolyte of the composition $70Li_2S{\cdot}30P_2S_5$ was shown. [69] describes the characteristics of a monolithic silicon electrode with a thickness of 1 μm in contact with an electrolyte with a garnet structure ($Li7La_3Zr_2O_{12}$ doped with 3 wt.% Al_2O_3). A specific capacity of 2685 mAh/g has been achieved here. An increase in the thickness of the electrode to 2 and 3 μm led to an expected decrease in capacity to 1700 and 830 mAh/g. Stable cycling of silicon electrodes with a columnar structure in contact with an argyrodite-like electrolyte of the composition Li_6PS_5Cl was reported in [70]. Similar results for electrodes made of silicon microparticles are given in [71–73]. The latest work also showed that the introduction of a small amount of LiI into the sulfide electrolyte leads to an increase in the elasticity of the electrolyte and protects silicon particles from destruction during lithiation-delithiation.

Electrodes in the form of films from a silicon-FeS mixture with a thickness of up to 1 μm in contact with the aforementioned sulfide glass-ceramic electrolyte demonstrated specific capacitance of 3000 and 2200 mAh/g when discharged in C/10 and 10 C modes [74].

It is known that when a sufficiently large amount of lithium is introduced into silicon, a significant increase in the specific volume occurs, leading to internal stresses and destruction of the material. To prevent this destruction, nanomaterials based on silicon and its alloys are widely used in traditional lithium-ion batteries with liquid electrolyte. A variety of nanoforms (nanopowders, nanofibers, thin films, etc.) are generally used. Multilayer structures in which thin layers of silicon are interspersed with layers of other materials are of particular interest [75–81]. Si-O-Al layered structures, which have proven themselves well in contact with the LiPON solid electrolyte, are described in [82–87]. Among other silicon-based composite materials used as negative electrodes in contact with solid electrolytes, composites with carbon [88], tin [89], and even such exotic materials as $Li_xTi_4Ni_4Si_7$ [90, 91] should be mentioned.

When using silicon in the form of micro- and nanopowders, a solid electrolyte is introduced into the active mass of the electrode [92, 93]. Amorphous silicon films also show a good ability to cycle in contact with a solid electrolyte [94, 95].

If silicon has the maximum specific capacity for the introduction of lithium, then lithium titanate $Li_4Ti_5O_{12}$ has the best cyclability. A distinctive feature of this material is the practical constancy of its specific volume during full lithiation (and reverse delithiation) and, as a result, the absence of internal stresses during cycling of the electrodes [96]. The process of reversible lithiation/delithiation is described by the equation

$$Li_4Ti_5O_{12} + 3\,e^- + 3\,Li^+ \leftrightarrow Li_7Ti_5O_{12}, \qquad (1)$$

therefore, the theoretical specific capacity of this process is 175 mAh/g. Lithium titanate, as such and in the form of various doped derivatives, is widely used in liquid electrolyte batteries. Examples of its use in contact with solid electrolytes are quite rare. In [97, 98], the characteristics of a model battery with a negative electrode made of lithium-indium alloy and a positive electrode made of $Li_4Ti_5O_{12}$ composite, a glass-ceramic electrolyte ($70Li_2S{\cdot}29P_2S_5{\cdot}1P_2S_3$) and an electrically conductive carbon fiber additive are given. The charging and discharging characteristics of such a model showed almost horizontal lines (which is typical for $Li_4Ti_5O_{12}$). The models withstood 700 cycles at a current density of 10 mA/cm^2 without noticeable degradation. The specific capacity of $Li_4Ti_5O_{12}$ in this case was 140 mAh/g. Models

of batteries with sulfide electrolytes of the compositions $Li_{9.54}Si_{1.74}P_{1.44}S_{11.7}Cl_{0.3}$ and $Li_{9.6}P_3S_{12}$ are described in [99]. In these models, a mixture of $LiCoO_4$ with an electrolyte and an electrically conductive additive (acetylene black) was used as the positive electrode, and a mixture of $Li_4Ti_5O_{12}$ composite with graphite, an electrolyte and an electrically conductive additive was used as the negative electrodes. It is reported that phenomenal results have been achieved: stable cycling of up to 1000 cycles in modes up to 0.9 C at a temperature of –30 °C and in modes up to 150 C and 1500 C at temperatures of 25 and 100 °C, respectively.

Materials for positive electrodes. The most popular active material for the positive electrodes of fully solid-state lithium-ion batteries remains lithium cobalt oxide $LiCoO_2$ (already mentioned in the references [20, 32, 40, 56, 63, 79, 99]. Unfortunately, deep cycling (dividing at potentials above 4.2 V, which means the extraction of approximately 50% or more of Li) leads to irreversible distortions of the $LiCoO_2$ crystal lattice from hexagonal to monoclinic symmetry, and this change worsens the cycling characteristics. In reality, only about 50% of lithium is extracted during cycling, that is, the electrode process is described by the equation

$$LiCoO_2 \leftrightarrow x\,Li^+ + x\,e + Li_{1-x}CoO_2, \qquad (2)$$

where $0<_x<0.5$.

The theoretical specific capacity of $LiCoO_2$ is 273 mAh/g, while the actual values do not exceed 140 mAh/g. Despite this, $LiCoO_2$ is still used in thin-film batteries with various solid electrolytes [100–114]. It was with such positive electrodes that flexible translucent batteries were created [100, 102]. However, the interaction of $LiCoO_2$ with sulfide electrolytes caused a certain problem [104–106]. Upon contact of these materials, mutual diffusion occurs and the formation of a kind of intermediate layer, which complicates interphase transport. One of the ways to combat this unpleasant phenomenon is to apply the thinnest (several monolayers) coating of various materials to the surface of the $LiCoO_2$ electrode, including Al_2O_3 [107], $LiNbO_3$ [108], $Li_4Ti_5O_{12}$ [109] and even Nb [110].

A radical method of increasing the specific capacity (i.e., the depth of cycling) of $LiCoO_2$-based electrodes, as well as reducing their cost, is the use of mixed lithium-containing oxides, i.e., lithium-cobalt oxides, in which some of the cobalt ions are replaced by ions of one or two other metals. Quite a lot of different multicomponent lithium oxides have been studied, of which the most popular are the $LiNi_xCo_yMn_zO_2$ (NMC) and $LiNi_xCo_yAl_zO_2$ (NCA) systems, including $LiNi_{1/3}Co_{1/3}Mn_{1/3}O_2$ and $LiNi_{0,8}Co_{0,15}Al_{0,05}O_2$ systems. Both materials are currently considered environmentally friendly, fairly cheap products with high specific capacity and good cyclability. NMC and NCA are very widely used in lithium-ion batteries with a liquid electrolyte, and examples of their use in fully solid-state batteries are limited (for instance, [115–119].

The theoretical specific capacity of NMC is 278 mAh/g, in practice it reaches up to 230 mAh/g. NMC has the same structure as $LiCoO_2$, i.e. it belongs to the type α-$NaFeO_2$ layered structure of rock salt. From a formal point of view, NMC can be considered as a solid solution of $LiCoO_2$-$LiNiO_2$-$LiMnO_2$ (1:1:1). In the initial state, nickel, cobalt, and manganese in NMC are in the 2+, 3+, and 4+ states, respectively, and Ni (2+/4+) and Co (3+/4+) transitions occur during cycling, and during the dilithiation, the Ni^{2+}/Ni^{3+} transition occurs first (with increasing $_x$ in the formula $Li_{1-x}[Co_{1/3}Ni_{1/3}Mn_{1/3}]O_2$ from 0 to 1/3), then the transition Ni^{3+}/Ni^{4+} (with x in the range $1/3 <x <2/3$) and finally Co^{3+}/Co^{4+} (with an increase in x from 2/3 to 1). It is this scheme of redox processes that provides the above value of the theoretical specific capacity.

The stable cycling of NMC is due to a slight change in the crystal lattice. When extracting 60% of the total amount of lithium contained in $LiNi_{1/3}Mn_{1/3}Co_{1/3}O_2$, the volume of the crystal cell does not change and amounts to 0.1 nm^3, and when it is almost completely removed, it decreases to only 0.095 nm^3.

The practical specific capacity of NCA also exceeds 200 mAh/g, and the cycling capacity of such electrodes is not inferior to traditional $LiCoO_2$-based electrodes.

Upon contact of both NMC and NCA with sulfide solid electrolytes, as in the case of $LiCoO_2$, a transition layer with increased resistance is also formed. Thin protective layers of various materials, including diamond-like carbon [115], $Li_4Ti_5O_{12}$ [116], and HfO_2 [118], are also applied to the surface of NMC and NCA.

In the initial period of the development of traditional lithium-ion batteries, lithium-manganese spinels of a composition close to $LiMn_2O_4$, as well as lithium-mixed nickel-manganese oxides, were widely used as the active material of the positive electrode. An important advantage of lithium-manganese spinels over other materials is their relatively low cost. Manganese compounds are much less toxic than cobalt compounds, and the manganese content in the earth's crust is also much higher than that of cobalt. In all-solid-state lithium-ion batteries, lithium manganese oxides are used much less [19, 62, 114, 120, 121], but with different types of electrolytes (LiPON [19, 62, 120], garnet type [114], phosphate [121]).

Electrodes made of lithium ferrophosphate ($LiFePO_4$), which belongs to the class of polyanionic compounds, are very widely used in batteries with liquid electrolyte. The theoretical specific capacity of $LiFePO_4$ is 170 mAh/g. The most important advantages of lithium ferrophosphate are relatively low cost, accessibility, non-toxicity, safety in operation, and most importantly, good cyclability. The main disadvantage is the extremely low electronic conductivity and low diffusion coefficient of lithium, which forces it to be used as a nanomaterial with a thin (about 3 nm) carbon coating, as well as to resort to doping with other cations, or fluoride and chloride anions.

The reversible process of lithium extraction and incorporation (during charging and discharging of the electrode) is described by a simple equation:

$$LiFePO_4 \leftrightarrow FePO_4 + Li^+ + e. \quad (3)$$

$LiFePO_4$ and $FePO_4$ are isostructural, so the course of reaction (3) is not accompanied by any structural changes, which ensures very good cycling of lithium ferrophosphate-based electrodes and the possibility of accelerated charges and discharges. The mutual solubility of $LiFePO_4$ and $FePO_4$ is insignificant, therefore, the process (3) proceeds according to a two-phase mechanism. In this respect, the $LiFePO_4/FePO_4$ system is very similar to the $Li_4Ti_5O_{12}/Li_7Ti_5O_{12}$ system described above. The galvanostatic curves obtained on lithium ferrophosphate electrodes also show almost horizontal sections (sections with constant potential) corresponding to the existence of two contacting phases $Li_\delta FePO_4$ and $Li_{1-\delta}FePO_4$. An example of using $LiFePO_4$-based electrodes in a solid electrolyte system is [122], which describes the design of a 3D battery with negative electrodes made of silicon nanorods, LiPON as an electrolyte, and a positive electrode made of a $LiFePO_4$ composite with carbon. Other examples of using $LiFePO_4$ are the works [123, 124]. The latter work is notable for the fact that it describes a mock-up of a lithium-ion battery in which a positive electrode from $LiFePO_4$ is combined with a negative electrode from $Li_3V_2(PO_4)_3$. Lithium vanadophosphate $Li_3V_2(PO_4)_3$ can function both as a negative electrode (then the V^{3+}/V^{2+} redox system with an operating potential of about 1.8 V (Li/Li^+) is implemented in it) and as a positive electrode (in this case, the V^{4+}/V^{3+} redox system with an operating potential is implemented, close to 4 V). The article [125] describes a symmetrical solid-state battery in which in the discharged state both electrodes have $Li_3V_2(PO_4)_3$. The electrolyte here is phosphate $Li_{1.5}Al_{0.5}Ge_{1.5}(PO_4)_3$ with the NASICON structure. When charged, one electrode is oxidized to $LiV_2(PO_4)_3$, and the other is reduced to $Li_5V_2(PO_4)_3$ with the transfer of two electrons and two Li^+ ions.

In general, the ability of vanadium to change its valence in oxide compounds in the range from +2 to +5 makes it tempting to use vanadium oxides as positive electrodes of lithium-ion batteries. Theoretically, the specific capacity of vanadium pentoxide can reach 883.5 mAh/g, which is much higher than the specific capacity of other compounds. Indeed, V_2O_5 was used in the first samples of fully solid-state lithium-ion batteries [18, 19, 126–128]. Unfortunately, the introduction of lithium into the crystal lattice of vanadium oxide is associated with significant structural changes. Even with the introduction of 2 moles of lithium per mole of V_2O_5, the γ-$Li_2V_2O_5$ phase appears with an irreversible change in structure. Unlike lithium ferrophosphate, vanadium oxide-based materials operate in a fairly wide range of potentials, which is a definite disadvantage.

Sulfides, including nickel sulfides [129, 130], titanium sulfides [131], and molybdenum sulfides [132], have become significantly less widespread as the active materials of the positive electrode of all-solid-state lithium-ion batteries.

PRODUCTION OF SOLID-STATE LITHIUM-ION BATTERIES

The scale of commercial production of fully solid-state lithium-ion batteries is still quite modest. In some cases, such production facilities existed for several years and then closed.

Cymbet Corp. (USA) produced miniature batteries (with overall dimensions of 1.7x2.25x 0.2 mm and 5.7x6.1.x0.2 mm) with a nominal capacity of 5 and 50 mAh. Front Edge Technology Inc. (USA) produced $LiCoO_2$|LiPON|Li batteries with dimensions of 25x20x0.1 mm and 25x20x0.3 mm with a capacity of 100 and 1000 mAh. Similar batteries with a capacity of 1000 mAh were manufactured by Infinity Power Solutions (USA), STMicroelectronics (France) and Excellatron (USA) [82].

It was reported [7] that Fujifilm Co. and Samsung produced batteries with sulfide electrolyte in a laminate case. Samsung batteries had a specific energy of 175 Wh/kg, they used positive electrodes based on NMC and negative electrodes based on graphite.

In 2016, Sony released batteries with LiPON electrolyte [7]. ProLogium Corporation (China) has announced the launch of ceramic electrolyte batteries with a specific energy of 810 Wh/l.

CONCLUSION

Despite the fact that all-solid-state thin-film lithium-ion batteries represent a special, relatively small category of batteries in terms of production

volume, the need for them has been increasing, especially in recent decades. This need is due to both the rapid development of microelectronics and high technologies in general, and the fundamental advantages of all-solid-state batteries in comparison with traditional batteries with liquid electrolytes (increased fire and explosion safety, the possibility of using lithium metal electrodes, the possibility of using technologies compatible with the manufacturing technology of integrated circuits and other semiconductor devices).

It would seem that such indisputable advantages would stimulate the development of large-scale production of all-solid-state lithium-ion batteries, however, as noted in the section "Production of solid-state lithium-ion batteries", only relatively small-sized products with a capacity of no more than 1 mAh have actually become production items. The reasons for this lag in industrial manufacturing, both from consumer demands and from the results of basic research, have been repeatedly discussed in the literature (see, for example, [2, 13, 133]). Along with the mentioned advantages of fully solid-state batteries, they also have certain disadvantages, in particular technological problems, and scaling, i.e. the transition to increasingly energy-intensive single products, is accompanied by increasing technological problems [134]. For example, the relatively low electronic conductivity of solid inorganic electrolytes dictates the need to minimize their thickness; at the same time, as the area of a single product increases, the risk of uneven thickness and other indicators increases markedly, as well as the risk of defects, in particular the appearance of through pores.

With an increase in the area of the electrodes in a single battery, the probability of local excess of the interfacial resistance at the interface of the electrode with a solid electrolyte increases markedly (which is impossible in systems with a liquid electrolyte) [135]. An increase in the size (and capacity) of individual products also encounters certain economic problems [136, 137].

Progress in the development of solid-state thin-film lithium-ion batteries is determined primarily by improvements in solid electrolytes, as well as improvements in functional electrode materials. In the future, we can expect the appearance of solid electrolytes with increased conductivity and a lithium transfer number close to unity. Of particular fundamental interest is the study of processes at the interface between an electrode and a solid electrolyte. Technologically, the development of 3D structures and the use of 3D printing is of particular interest.

FUNDING

The work was carried out with the financial support of the Ministry of Science and Higher Education of the Russian Federation.

CONFLICT OF INTEREST

The authors declare that there is no conflict of interest.

REFERENCES

1. Kulova, T., Mironenko, A., Rudy, A., and Skundin, A. *All Solid State Thin-Film Lithium-Ion Batteries: Materials, Technology, and Diagnostics,* CRC Press. Taylor & Francis Group. 2021. 214 p. ISBN 9780367086824
2. Guo, Y., Wu, S., He, Y., Kang, F., Chen, L., Li, H., and Yang, Q., Solid-state lithium batteries: Safety and prospects, *eScience*, 2022, vol. 2, p. 138. https://doi.org/10.1016/j.esci.2022.02.008
3. Patil, A., Patil, V., Shin, D.W., Choi, J., Paik, D., and Yoon, S., Issue and challenges facing rechargeable thin film lithium batteries, *Mat. Res. Bull.*, 2008, vol. 43, p. 1913. doi:10.1016/j.materresbull.2007.08.031
4. Oudenhoven, J.F.M., Baggetto, L., and Notten, P.H.L., All-Solid-State Lithium-Ion Microbatteries: A Review of Various Three-Dimensional Concepts, *Adv. Energy Mater.*, 2011, vol. 1, p. 10. https://doi.org/10.1002/aenm.201000002
5. Zhou, Y., Xue, M., and Fu, Z., Nanostructured thin film electrodes for lithium storage and all-solid-state thin-film lithium batteries, *J. Power Sources*, 2013, vol. 234, p. 310. http://dx.doi.org/10.1016/j.jpowsour.2013.01.183
6. Ko, J., and Yoon, Y.S., Lithium phosphorus oxynitride thin films for rechargeable lithium batteries: Applications from thin-film batteries as micro batteries to surface modification for large-scale batteries, *Ceram. Int.*, 2022, vol. 48, p. 10372. https://doi.org/10.1016/j.ceramint.2022.02.173
7. Sun, C., Liu, J., Gong, Y., Wilkinsone, D.P., and Zhang, J., Recent advances in all-solid-state rechargeable lithium batteries, *Nano Energy*, 2017, vol. 33, p. 363. http://dx.doi.org/10.1016/j.nanoen.2017.01.028
8. Patil, A., Patil, V., Choi, J., Kim, J., and Yoon, S., Solid Electrolytes for Rechargeable Thin Film Lithium Batteries: A Review, *J. Nanosci. Nanotechnol.*, 2017, vol. 17, p. 29. DOI:10.1166/jnn.2017.12699
9. Xu, R.C., Xia, X.H., Zhang, S.Z., Xie, D., Wang, X.L., and Tu, J.P., Interfacial challenges and progress for inorganic all-solid-state lithium batteries, *Electrochim. Acta,* 2018, vol. 284, p. 177. https://doi.org/10.1016/j.electacta.2018.07.191
10. Moitzheim, S., Put, B., and Vereecken, P.M., Advances in 3D Thin-Film Li-Ion Batteries, *Adv. Mater. Interfaces,* 2019, vol. 6, article # 1900805. DOI: 10.1002/admi.201900805

11. Clement, B., Lyu, M., Kulkarni, E.S., Lin, T., Hua, Y., Lockett, V., Greig, C., and Wanga, L., Recent Advances in Printed Thin-Film Batteries, *Engineering,* 2022, vol. 13, article # 238. https://doi.org/10.1016/j.eng.2022.04.002

12. Yu, Y., Gong, M., Dong, C., and Xu, X., Thin-film deposition techniques in surface and interface engineering of solid-state lithium batteries, *Next Nanotechnol.*, 2023, vol. 3–4, article # 100028. https://doi.org/10.1016/j.nxnano.2023.100028

13. Machín, A., Morant, C., and Márquez, F., Advancements and Challenges in Solid-State Battery Technology: An In-Depth Review of Solid Electrolytes and Anode Innovations, *Batteries*, 2023, vol. 10, article # 29. https://doi.org/10.3390/batteries10010029

14. Jetybayeva, A., Aaron, D.S., Belharouak, I., and Mench, M.M., Critical review on recently developed lithium and non-lithium anode-based solid-state lithium-ion batteries, *J. Power Sources*, 2023, vol. 566, article # 232914. https://doi.org/10.1016/j.jpowsour.2023.232914

15. Wu, D., Chen, L., Li, H., and Wu, F., Solid-state lithium batteries-from fundamental research to industrial progress, *Prog. Mater. Sci.*, 2023, vol. 139, article # 101182. https://doi.org/10.1016/j.pmatsci.2023.101182

16. Shalaby, M.S., Alziyadi, M.O., Gamal, H., and Hamdy, S., Solid-state lithium-ion battery: The key components enhance the performance and efficiency of anode, cathode, and solid electrolytes, *J. Alloys Comp.*, 2023, vol. 969, article # 172318. https://doi.org/10.1016/j.jallcom.2023.172318

17. Bates, J.B., Dudney, N.J., Gruzalski, G.R., Zuhr, R.A., Choudhury, A., Luck, C.F., and Robertson, J.D., Electrical properties of amorphous lithium electrolyte thin films, *Solid State Ionics*, 1992, vol. 53–56, p. 647. https://doi.org/10.1016/0167–2738(92)90442-R

18. Bates, J.B., Dudney, N.J., Gruzalski, G.R., Zuhr, R.A., Choudhury, A., Luck, C.F., and Robertson, J.D., Fabrication and characterization of amorphous lithium electrolyte thin films and rechargeable thin-film batteries, *J. Power Sources,* 1993, vol. 43/44, p. 103. https://doi.org/10.1016/0378–7753(93)80106-Y

19. Bates, J.B., Dudney, N.J., Lubben, D.C., Gruzalski, G.R., Kwak, B.S., Yu, X., and Zuhr, R.A., Thin-film rechargeable lithium batteries, *J. Power Sources,* 1995, vol. 54, p. 58. https://doi.org/10.1016/0378–7753(94)02040-A

20. Wang, B., Bates, J.B., Hart, F.X., Sales, B.C., Zuhr, R.A., and Robertson, J.D., Characterization of Thin-Film Rechargeable Lithium Batteries with Lithium Cobalt Oxide Cathodes, *J. Electrochem. Soc.*, 1996, vol. 143, p. 3203. DOI 10.1149/1.1837188

21. Notten, P.H.L., Roozeboom, F., Niessen, R.A.H., and Baggetto, L., 3-D Integrated All-Solid-State Rechargeable Batteries, *Adv. Mater.*, 2007, vol. 19, p. 4564. DOI: 10.1002/adma.200702398

22. Ferrari, S., Loveridge, M., Beattie, S.D., Jahn, M., Dashwood, R.J., and Bhagat, R., Latest advances in the manufacturing of 3D rechargeable lithium microbatteries. *J. Power Sources*, 2015, vol. 286, p. 25. http://dx.doi.org/10.1016/j.jpowsour.2015.03.133

23. Long, J.W., Dunn, B., Rolison, D.R., and White, H.S., Three-dimensional battery architectures, *Chem. Rev.,* 2004, vol. 104, p. 4463. https://doi.org/10.1021/cr020740l

24. Edstrom, K., Brandell, D., Gustafsson, T., and Nyholm, L., Electrodeposition as a Tool for 3D Microbattery Fabrication, *Interface*, 2011, vol. 20, no. 2, p. 41. DOI 10.1149/2.F05112if [open access]

25. Roberts, M., Johns, P., Owen, J., Brandell, D., Edstrom, K., El Enany, G., Guery, C., Golodnitsky, D., Lacey, M., Lecoeur, C., Mazor, H., Peled, E., Perre, E., Shaijumon, M.M., Simon, P., and Taberna, P.-L., 3D lithium ion batteries – from fundamentals to fabrication, *J. Mater. Chem.*, 2011, vol. 21, p. 9876. DOI: 10.1039/c0jm04396f

26. Arthur, T.S., Bates, D.J., Cirigliano, N., Johnson, D.C., Malati, P., Mosby, J.M., Perre, E., Rawls, M.T., Prieto, A.L., and Dunn, B., Three-dimensional electrodes and battery architectures, *MRS Bull.*, 2011, vol. 36, p. 523. https://doi.org/10.1557/mrs.2011.156

27. Rolison, D.R., Long, J.W., Lytle, J.C., Fischer, A.E., Rhodes, C.P., McEvoy, T.M., Bourga, M.E., and Lubers, A.M., Multifunctional 3D nanoarchitectures for energy storage and conversion, *Chem. Soc. Rev.*, 2009, vol. 38, p. 226. https://doi.org/10.1039/B801151F

28. Zhang, F., Wei, M., Viswanathan, V.V., Swart, B., Shao, Y., Wu, G., and Zhou, C., 3D printing technologies for electrochemical energy storage, *Nano Energy*, 2017, vol. 40, p. 418. http://dx.doi.org/10.1016/j.nanoen.2017.08.037

29. Sun, K., Wei, T.-S., Ahn, B.Y., Seo, J.Y., Dillon, S.J., and Lewis, J.A., 3D Printing of Interdigitated Li-Ion Microbattery Architectures, *Adv. Mater.*, 2013, vol. 25, p. 4539. DOI: 10.1002/adma.201301036

30. Wei, M., Zhang, F., Wang, W., Alexandridis, P., Zhou, C., and Wu, G., 3D direct writing fabrication of electrodes for electrochemical storage devices, *J. Power Sources*, 2017, vol. 354, p. 134. http://dx.doi.org/10.1016/j.jpowsour.2017.04.042

31. Yang, Y., Jeong, S., Hu, L., Wu, H., Lee, S.W., and Cui, Y., Transparent Lithium-Ion Batteries, *Proc. Natl. Acad. Sci. U.S.A.,* 2011, vol. 108, p. 13013. www.pnas.org/cgi/doi/10.1073/pnas.1102873108

32. Oukassi, S., Baggetto, L., Dubarry, C., Le Van-Jodin, L., Poncet, S., and Salot, R., Transparent Thin Film Solid-State Lithium Ion Batteries, *ACS Appl. Mater. Interfaces*, 2019, vol. 11, p. 683. DOI: 10.1021/acsami.8b16364

33. Zhang, Z., Shao, Y., Lotsch, B., Hu, Y.S., Li, H., Janek, J., Nazar, L.F., Nan, C., Maier, J., Armand, M., and Chen, L., New horizons for inorganic solid state

ion conductors, *Energy Environ. Sci.*, 2018, vol. 11, p. 1945. DOI: 10.1039/c8ee01053f

34. Takada, K., Progress in solid electrolytes toward realizing solid-state lithium batteries, *J. Power Sources*, 2018, vol. 394, p. 74. https://doi.org/10.1016/j.jpowsour.2018.05.003
35. Campanella, D., Belanger, D., and Paolella, A., Beyond garnets, phosphates and phosphosulfides solid electrolytes: New ceramic perspectives for all solid lithium metal batteries, *J. Power Sources*, 2021, vol. 482, article # 228949. https://doi.org/10.1016/j.jpowsour.2020.228949
36. Thangadurai, V., Narayanan, S., and Pinzaru, D., Garnet-type solid-state fast Li ion conductors for Li batteries: critical review, *Chem. Soc. Rev.*, 2014, vol. 43, p. 4714. DOI: 10.1039/c4cs00020j
37. Guo, R., Zhang, K., Zhao, W., Hu, Z., Li, S., Zhong, Y., Yang, R., Wang, X., Wang, J., Wu, C., and Bai, Y., Interfacial Challenges and Strategies toward Practical Sulfide-Based Solid-State Lithium Batteries, *Energy Mater. Adv.*, 2023, vol. 4, article #0022. https://doi.org/10.34133/energymatadv.0022
38. Liu, D., Zhu, W., Feng, Z., Guerfi, A., Vijh, A., and Zaghib, K., Recent progress in sulfide-based solid electrolytes for Li-ion batteries, *Mat. Sci. Eng. B*, 2016, vol. 213, p. 169. http://dx.doi.org/10.1016/j.mseb.2016.03.005
39. Zhang, X., Wang, J., Hu, D., Du, W., Hou, C., Jiang, H., Wei, Y., Liu, X., Jiang, F., Sun, J., Yuan, H., and Huang, X., High-performance lithium metal batteries based on composite solid-state electrolytes with high ceramic content, *Energy Storage Mater.*, 2024, vol. 65, article # 103089. https://doi.org/10.1016/j.ensm.2023.103089
40. Zhang, Z., Wang, X., Li, X., Zhao, J., Liu, G., Yu, W., Dong, X., and Wang, J., Review on composite solid electrolytes for solid-state lithium-ion batteries, *Mater. Today Sustainability*, 2023, vol. 21, article # 100316. https://doi.org/10.1016/j.mtsust.2023.100316
41. Devaraj, L., Thummalapalli, S.V., Fonseca, N., Nazir, H., Song, K., and Kannan, A.M., Comprehending garnet solid electrolytes and interfaces in all-solid lithium-ion batteries, *Mater. Today Sustainability*, 2024, vol. 25, article # 100614. https://doi.org/10.1016/j.mtsust.2023.100614
42. Han, Y., Chen, Y., Huang, Y., Zhang, M., Li, Z., and Wang, Y., Recent progress on garnet-type oxide electrolytes for all-solid-state lithium-ion batteries, *Ceram. Int.*, 2023, vol. 49, p. 29375. https://doi.org/10.1016/j.ceramint.2023.06.153
43. Joo, K.H., Sohn, H.J., Vinatier, P., Pecquenard, B., and Levasseur, A., Lithium Ion Conducting Lithium Sulfur Oxynitride Thin Film, *Electrochem. Solid State Lett.,* 2004, vol. 7, p. A256. DOI: 10.1149/1.1769317
44. Jones, S.D., Akridge, J.R., and Shokoohi, F.K., Thin film rechargeable Li batteries, *Solid State Ionics*, 1994, vol. 69, p. 357. https://doi.org/10.1016/0167–2738(94)90423–5
45. Ujiie, S., Hayashi, A., and Tatsumisago, M., Preparation and ionic conductivity of (100-x)($0.8Li_2S_{0.2}P_2S_5$)·xLiI glass–ceramic electrolytes, *J. Solid State Electrochem.*, 2013, vol. 17, p. 675. https://doi.org/10.1007/s10008–012–1900–7
46. Jung, W.D., Kim, J., Choi, S., Kim, S., Jeon, M., Jung, H., Chung, K.Y., Lee, J., Kim, B., Lee, J., and Kim, H., Superionic Halogen-Rich Li-Argyrodites Using In Situ Nanocrystal Nucleation and Rapid Crystal Growth, *Nano Lett.*, 2020, vol. 20, p. 2303. https://doi.org/10.1021/acs.nanolett.9b04597
47. Zhang, Z., Wu, L., Zhou, D., Weng, W., and Yao, X., Flexible Sulfide Electrolyte Thin Membrane with Ultrahigh Ionic Conductivity for All-Solid-State Lithium Batteries, *Nano Lett.*, 2021, vol. 21, p. 5233. https://doi.org/10.1021/acs.nanolett.1c01344
48. Fu, J., Superionic conductivity of glass-ceramics in the system $Li_2O–Al_2O_3–TiO_2–P_2O_5$, *Solid State Ionics*, 1997, vol. 96, p. 195. https://doi.org/10.1016/S0167–2738(97)00018–0
49. Mizuno, F., Hayashi, A., Tadanaga, K., and Tatsumisago, M., New, Highly Ion-Conductive Crystals Precipitated from $Li_2S–P_2S_5$ Glasses, *Adv. Mater.*, 2005, vol. 17, p. 918. DOI:10.1002/adma.200401286
50. Tatsumisago, M., Glassy materials based on Li_2S for all-solid-state lithium secondary batteries, *Solid State Ionics*, 2004, vol. 175, p. 13. https://doi.org/10.1016/j.ssi.2004.09.012
51. Seino, Y., Ota, T., Takada, K., Hayashi, A., and Tatsumisago, M., A sulphide lithium super ion conductor is superior to liquid ion conductors for use in rechargeable batteries, *Energy Environ. Sci.*, 2014, vol. 7, p. 627. DOI: 10.1039/c3ee41655k
52. Stramare, S., Thangadurai, V., and Weppner, W., Lithium Lanthanum Titanates: A Review, *Chem. Mater.*, 2003, vol. 15, p. 3974. https://doi.org/10.1021/cm0300516
53. Bohnke, O., The fast lithium-ion conducting oxides $Li_{3x}La_{2/3-x}TiO_3$ from fundamentals to application, *Solid State Ionics*, 2008, vol. 179, p.9. DOI: 10.1016/j.ssi.2007.12.022
54. Kanno, R. and Murayama, M., Lithium Ionic Conductor Thio-LISICON: The $Li_2S–GeS_2–P_2S_5$ System, *J. Electrochem. Soc.*, 2001, vol. 148, p. A742. DOI 10.1149/1.1379028
55. Takada, K., Inada, T., Kajiyama, A., Sasaki, H., Kondo, S., Watanabe, M., Murayama, M., and Kanno, R., Solid-state lithium battery with graphite anode, *Solid State Ionics*, 2003, vol. 158, p. 269. https://doi.org/10.1016/S0167–2738(02)00823–8
56. Kamaya, N., Homma, K., Yamakawa, Y., Hirayama, M., Kanno, R., Yonemura, M., Kamiyama, T., Kato, Y., Hama, S., Kawamoto, K., and Matsui, A., A lithium superionic conductor, *Nat. Mater.*, 2011, vol. 10, p. 682. DOI: 10.1038/NMAT3066

57. Murugan, R., Weppner, W., Schmid-Beurmann, P., and Thangadurai, V., Structure and lithium ion conductivity of bismuth containing lithium garnets $Li_5La_3Bi_2O_{12}$ and $Li_6SrLa_2Bi_2O_{12}$, *Mater. Sci. Eng. B.,* 2007, vol. 143, p. 14. https://doi.org/10.1016/j.mseb.2007.07.009

58. Ohta, S., Kobayashi, T., and Asaoka, T., High lithium ionic conductivity in the garnet type oxide $Li_{7-X}La_3(Zr_{2-X}, Nb_X)O_{12}$, *J. Power Sources*, 2011, vol. 196, p. 3342. https://doi.org/10.1016/j.jpowsour.2010.11.089

59. El Shinawi, H. and Janek, J., Stabilization of cubic lithium-stuffed garnets of the type ''$Li_7La_3Zr_2O_{12}$'' by addition of gallium, *J. Power Sources*, 2013, vol. 225, p. 13. https://doi.org/10.1016/j.jpowsour.2012.09.111

60. Allen, J.L., Wolfenstine, J., Rangasamy, E., and Sakamoto, J., Effect of substitution (Ta, Al, Ga) on the conductivity of $Li_7La_3Zr_2O_{12}$, *J. Power Sources*, 2012, vol. 206, p. 315. https://doi.org/10.1016/j.jpowsour.2012.01.131

61. Shen, Y., Zhang, Y., Han, S., Wang, J., Peng, Z., and Chen L., Unlocking the Energy Capabilities of Lithium Metal Electrode with Solid-State Electrolytes, *Joule*, 2018, vol. 2, p. 1674. https://doi.org/10.1016/j.joule.2018.06.021

62. Dudney, N., Thin film micro-batteries, *Interface*, 2008, no. 3, p. 44. DOI: 10.1149/2.F04083IF

63. Neudecker, B.J., Dudney, N.J., and Bates, J.B., "Lithium-Free" Thin-Film Battery with in situ Plated Li Anode, *J. Electrochem. Soc.*, 2000, vol. 147, p. 517. DOI: 10.1149/1.1393226

64. Baggetto, L., Niessen, R.A.H., and Notten, P.H.L., On the activation and charge transfer kinetics of evaporated silicon electrode/electrolyte interfaces, *Electrochim. Acta*, 2009, vol. 54, p. 5937. DOI:10.1016/j.electacta.2009.05.070

65. Phan, V.P., Pecquenard, B., and Le Cras, F., High-Performance All-Solid-State Cells Fabricated With Silicon Electrodes, *Adv. Funct. Mater.*, 2012, vol. 22, p. 2580. https://doi.org/10.1002/adfm.201200104

66. Sakabe, J., Ohta, N., Ohnishi, T., Mitsuishi, K., and Takada, K., Porous amorphous silicon film anodes for high-capacity and stable all-solid-state lithium batteries, *Commun. Chem.*, 2018, vol. 1, article # 24. https://doi.org/10.1038/s42004–018–0026-y

67. Miyazaki, R., Ohta, N., Ohnishi, T., Sakaguchi, I., and Takada, K., An amorphous Si film anode for all-solid-state lithium batteries, *J. Power Sources,* 2014, vol. 272, p. 541. http://dx.doi.org/10.1016/j.jpowsour.2014.08.109

68. Miyazaki, R., Ohta, N., Ohnishi, T., and Takada, K., Anode properties of silicon-rich amorphous silicon suboxide films in all-solid-state lithium batteries, *J. Power Sources,* 2016, vol. 329, p. 41. http://dx.doi.org/10.1016/j.jpowsour.2016.08.070

69. Ping, W., Yang, C., Bao, Y., Wang, C., Xie, H., Hitz, E., Cheng, J., Li, T., and Hu, L., A silicon anode for garnet-based all-solid-state batteries: Interfaces and nanomechanics, *Energy Storage Mater.*, 2019, vol. 21, p. 246. https://doi.org/10.1016/j.ensm.2019.06.024

70. Cangaz, S., Hippauf, F., Reuter, F.S., Doerfler, S., Abendroth, T., Althues, H., and Kaskel, S., Enabling High-Energy Solid-State Batteries with Stable Anode Interphase by the Use of Columnar Silicon Anodes, *Adv. Energy Mater.*, 2020, vol. 10, article # 2001320. DOI: 10.1002/aenm.202001320

71. Tan, D.H.S., Chen, Y., Yang, H., Bao, W., Sreenarayanan, B., Doux, J., Li, W., Lu, B., Ham, S., Sayahpour, B., Scharf, J., Wu, E.A., Deysher, G., Han, H.E., Hah, H.J., Jeong, H., Lee, J.B., Chen, Z., and Meng, Y.S., Carbon-free high-loading silicon anodes enabled by sulfide solid electrolytes, *Science*, 2021, vol. 373, p.1494. DOI: 10.1126/science.abg7217

72. Okuno, R., Yamamoto, M., Terauchi, Y., and Takahashi, M., Stable cyclability of porous Si anode applied for sulfide-based all solid-state batteries, *ACS Appl. Energy Mater.*, 2019, vol. 2, p. 7005. DOI: 10.1021/acsaem.9b01517

73. Kato, A., Yamamoto, M., Sakuda, A., Hayashi, A., and Tatsumisago, M., Mechanical properties of $Li_2S–P_2S_5$ glasses with lithium halides and application in all-solid-state batteries, *ACS Appl. Energy Mater.*, 2018, vol. 1, p. 1002. DOI: 10.1021/acsaem.7b00140

74. Cervera, R.B., Suzuki, N., Ohnishi, T., Osada, M., Mitsuishi, K., Kambara, T., and Takada, K., High performance silicon-based anodes in solid-state lithium batteries, *Energy Environ. Sci.*, 2014, vol. 7, p. 662. https://doi.org/10.1039/c3ee43306d

75. Roginskaya, Yu.E., Kulova, T.L., Skundin, A.M., Bruk, M.A., Klochikhina, A.V., Kozlova, N.V., Kal'nov, V.A., and Loginov, B.A., The Structure and Properties of a New Type of Nanostructured Composite Si/C Electrodes for Lithium Ion Accumulators, *Russ. J. Phys. Chem. A*, 2008, vol. 82, p. 1655. DOI: 10.1134/S0036024408100063

76. Roginskaya, Yu.E., Kulova, T.L., Skundin, A.M., Bruk, M.A., Zhikharev, E.N., Kal'nov, V.A., and Loginov, B.A., New Type of the Nanostructured Composite Si/C Electrodes, *Russ. J. Electrochem.*, 2008, vol. 44, p. 1197. DOI: 10.1134/S1023193508110025

77. Li, W., Yang, R., Wang, X., Wang, T., Zheng, J., and Li, X.J., Intercalated Si/C films as the anode for Li-ion batteries with near theoretical stable capacity prepared by dual plasma deposition, *J. Power Sources*, 2013, vol. 221, p. 242. https://doi.org/10.1016/j.jpowsour.2012.08.042

78. Kim, J.-B., Lim, S.-H., and Lee, S.-M., Structural Change in Si Phase of Fe/Si Multilayer Thin-Film Anodes during Li Insertion/Extraction Reaction, *J. Electrochem. Soc.*, 2006, vol. 153, p. A455. DOI: 10.1149/1.2158567

79. Hwang, C.-M. and Park, J.-W., Electrochemical characterizations of multi-layer and composite silicon–germanium anodes for Li-ion batteries using magnetron

sputtering, *J. Power Sources,* 2011, vol. 196, p. 6772. https://doi.org/10.1016/j.jpowsour.2010.10.061

80. Demirkan, M.T., Trahey, L., and Karabacak, T., Cycling performance of density modulated multilayer silicon thin film anodes in Li-ion batteries, *J. Power Sources,* 2015, vol. 273, p. 52. https://doi.org/10.1016/j.jpowsour.2014.09.027
81. Demirkan, M.T., Yurukcu, M., Dursun, B., Demir-Cakan, R., and Karabacak, T., Evaluation of double-layer density modulated Si thin films as Li-ion battery anodes, *Mater. Res. Express*, 2017, vol. 4, article # 106405. https://doi.org/10.1088/2053–1591/aa8f88
82. Rudyi, A.S., Mironenko, A.A., Naumov, V.V., Skundin, A.M., Kulova, T.L., Fedorov, I.S., and Vasil'ev, S.V., A Solid-State Lithium-Ion Battery: Structure, Technology, and Characteristics, *Tech. Phys. Lett*., 2020, vol. 46, no. 3, p. 217. DOI: 10.1134/S1063785020030141
83. Kulova, T.L., Mazaletsky, L.A., Mironenko, A.A., Rudy, A.S., Skundin, A.M., Tortseva, Yu.S., and Fedorov, I.S., Experimental Study of the Influence of the Porosity of Thin-Film Silicon-Based Anodes on Their Charge-Discharge Characteristics, *Russ. Microelectron*., 2021, vol. 50, no. 1, p. 45. DOI: 10.1134/S1063739720060074
84. Rudy, A.S., Mironenko, A.A., Naumov, V.V., Fedorov, I.S., Skundin, A.M., and Tortseva, Yu.S., Thin-Film Solid State Lithium-Ion Batteries of the $LiCoO_2$/Lipon/Si@O@Al System, *Russ. Microelectron*., 2021, vol. 50, no. 5, p. 333. DOI: 10.1134/S106373972105005X
85. Kurbatov, S., Mironenko, A., Naumov, V., Skundin, A., and Rudy, A., Effect of the Etching Profile of a Si Substrate on the Capacitive Characteristics of Three-Dimensional Solid-State Lithium-Ion Batteries, *Batteries,* 2021, vol. 7, Article # 65. https://doi.org/10.3390/batteries7040065
86. Rudy, A.S., Kurbatov, S.V., Mironenko, A.A., Naumov, V.V., Skundin, A.M., and Egorova, Yu.S., Effect of Si-Based Anode Lithiation on Charging Characteristics of All-Solid-State Lithium-Ion Battery, *Batteries*, 2022, vol. 8, Article # 87. https://doi.org/10.3390/batteries8080087
87. Rudy, A.S., Skundin, A.M., Mironenko, A.A., and Naumov, V.V., Current Effect on the Performances of All-Solid-State Lithium-Ion Batteries – Peukert's Law, *Batteries,* 2023, vol. 9, article # 370. https://doi.org/10.3390/batteries9070370
88. Dunlap, N.A, Kim, S., Jeong, J.J., Oh, K.H., and Lee, S., Simple and inexpensive coal-tar-pitch derived Si-C anode composite for all solid-state Li-ion batteries, *Solid State Ionics*, 2018, vol. 324, p. 207. https://doi.org/10.1016/j.ssi.2018.07.013
89. Whiteley, J.M., Kim, J.W., Piper, D.M., and Se-Hee Lee, S., High-Capacity and Highly Reversible Silicon-Tin Hybrid Anode for Solid-State Lithium-Ion Batteries, *J. Electrochem. Soc.*, 2016, vol. 163, p. A251. DOI: 10.1149/2.0701602jes
90. Son, S.B., Kim, S.C., Kang, C.S., Yersak, T.A., Kim, Y.C., Lee, C.G., Moon, S.H., Cho, J.S., Moon, J.T., Oh, K.H., and Lee, S.H., A Highly Reversible Nano-Si Anode Enabled by Mechanical Confinement in an Electrochemically Activated $Li_xTi_4Ni_4Si_7$ Matrix, *Adv. Energy Mater.*, 2012, vol. 2, p. 1226. DOI: 10.1002/aenm.201200180
91. Yersak, T.A., Son, S.B., Cho, J.S., Suh, S.S., Kim, Y.U., Moon, J.T., Oh, K.H., and Lee, S.H., An All-Solid-State Li-Ion Battery with a Pre-Lithiated Si-Ti-Ni Alloy Anode, *J. Electrochem. Soc.*, 2013, vol. 160, p. A1497. DOI: 10.1149/2.086309jes
92. Yamamoto, M., Terauchi, Y., Sakuda, A., and Takahashi, M., Slurry mixing for fabricating silicon-composite electrodes in all-solid-state batteries with high areal capacity and cycling stability, *J. Power Sources*, 2018, vol. 402, p. 506. https://doi.org/10.1016/j.jpowsour.2018.09.070
93. Kim, D.H., Lee, H.A., Song, Y.B., Park, J.W., Lee, S., and Jung, Y.S., Sheet-type Li_6PS_5Cl-infiltrated Si anodes fabricated by solution process for all-solid-state lithium-ion batteries, *J. Power Sources*, 2019, vol. 426, p. 143. https://doi.org/10.1016/j.jpowsour.2019.04.028
94. Kanazawa, S., Baba, T., Yoneda, K., Mizuhata, M., and Kanno, I., Deposition and performance of all solid-state thin-film lithium-ion batteries composed of amorphous Si/LiPON/VO-LiPO multilayers, *Thin Solid Films*, 2020, vol. 697, article # 137840. https://doi.org/10.1016/j.tsf.2020.137840
95. Chai, L., Wang, X., Su, B., Li, X., and Xue, W., Insight into the decay mechanism of non-ultra-thin silicon film anode for lithium-ion batteries, *Electrochim. Acta*, 2023, vol. 448, article # 142112. https://doi.org/10.1016/j.electacta.2023.142112
96. Ohzuku, T., Ueda, A., and Yamamoto, N., Zero-Strain Insertion Material of $Li[Li_{1/3}Ti_{5/3}]O_4$ for Rechargeable Lithium Cells, *J. Electrochem. Soc.*, 1995, vol. 142, p. 1431. DOI: 10.1149/1.2048592
97. Minami, K., Hayashi, A., Ujiie, S., and Tatsumisago, M., Electrical and electrochemical properties of glass–ceramic electrolytes in the systems Li_2S–P_2S_5–P_2S_3 and Li_2S–P_2S_5–P_2O_5, *Solid State Ionics*, 2011, vol. 192, p. 122. DOI:10.1016/j.ssi.2010.06.018
98. Tatsumisago, M., and Hayashi, A., Superionic glasses and glass–ceramics in the Li_2S–P_2S_5 system for all-solid-state lithium secondary batteries, *Solid State Ionics*, 2012, vol. 225, p. 342. DOI: 10.1016/j.ssi.2012.03.013
99. Kato, Y., Hori, S., Saito, T., Suzuki, K., Hirayama, M., Mitsui, A., Yonemura, M., Iba, H., and Kanno, R., High-power all-solid-state batteries using sulfide superionic conductors, *Nano Energy*, 2016, vol. 1, article # 16030. DOI: 10.1038/NENERGY.2016.30
100. Song, S., Hong, S., Park, H.Y., Lim, Y.C., and Lee, K.C., Cycling-Driven Structural Changes

in a Thin-Film Lithium Battery on Flexible Substrate, *Electrochem. Solid-State Lett.*, 2009, vol. 12, p. A159. DOI: 10.1149/1.3139530

101. Yamamoto, T., Iwasaki, H., Suzuki, Y., Sakakura, M., Fujii, Y., Motoyama, M., and Iriyama, Y., A Li-free inverted-stack all-solid-state thin film battery using crystalline cathode material, *Electrochem. Commun.*, 2019, vol. 105, article # 106494. https://doi.org/10.1016/j.elecom.2019.106494
102. Koo, M., Park, K., Lee, S.H., Suh, M., Jeon, D.Y., Choi, J.W., Kang, K., and Lee, K.J., Bendable Inorganic Thin-Film Battery for Fully Flexible Electronic Systems, *Nano Lett.*, 2012, vol. 12, p. 4810. dx.doi.org/10.1021/nl302254v
103. Xiao, D., Tong, J., Feng, Y., Zhong, G., Li, W., and Yang, C., Improved performance of all-solid-state lithium batteries using LiPON electrolyte prepared with Li-rich sputtering target, *Solid State Ionics*, 2018, vol. 324, p. 202. https://doi.org/10.1016/j.ssi.2018.07.011
104. Haruyama, J., Sodeyama, K., Han, L., Takada, K., and Tateyama, Y., Space–Charge Layer Effect at Interface between Oxide Cathode and Sulfide Electrolyte in All-Solid-State Lithium-Ion Battery, *Chem. Mater.*, 2014, vol. 26, p. 4248. https://doi.org/10.1021/cm5016959
105. Haruyama, J., Sodeyama, K., and Tateyama, Y., Cation Mixing Properties toward Co Diffusion at the $LiCoO_2$ Cathode/Sulfide Electrolyte Interface in a Solid-State Battery, *ACS Appl. Mater. Interfaces,* 2017, vol. 9, p. 286. DOI: 10.1021/acsami.6b08435
106. Sakuda, A., Hayashi, A., and Tatsumisago, M., Interfacial Observation between $LiCoO_2$ Electrode and Li_2S-P_2S_5 Solid Electrolytes of All-Solid-State Lithium Secondary Batteries Using Transmission Electron Microscopy, *Chem. Mater.*, 2010, vol. 22, p. 949. DOI: 10.1021/cm901819c
107. Woo, J.H., Trevey, J.E., Cavanagh, A.S., Choi, Y.S., Kim, S.C., George, S.M., Oh, K.H., and Lee, S., Nanoscale Interface Modification of $LiCoO_2$ by Al_2O_3 Atomic Layer Deposition for Solid-State Li Batteries, *J. Electrochem. Soc.*, 2012, vol. 159, p. A1120. DOI: 10.1149/2.085207jes
108. Ohta, N., Takada, K., Sakaguchi, I., Zhang, L., Ma, R., Fukuda, K., Osada, M., and Sasaki, T., $LiNbO_3$-coated $LiCoO_2$ as cathode material for all solid-state lithium secondary batteries, *Electrochem. Commun.*, 2007, vol. 9, p. 1486. DOI: 10.1016/j.elecom.2007.02.008
109. Ohta, N., Takada, K., Zhang, L., Ma, R., Osada, M., and Sasaki, T., Enhancement of the High-Rate Capability of Solid-State Lithium Batteries by Nanoscale Interfacial Modification, *Adv. Mater.*, 2006, vol. 18, p. 2226. DOI: 10.1002/adma.200502604
110. Kato, T., Hamanaka, T., Yamamoto, K., Hirayama, T., Sagane, F., Motoyama, M., and Iriyama, Y., *In-situ* $Li_7La_3Zr_2O_{12}/LiCoO_2$ interface modification for advanced all-solid-state battery, *J. Power Sources*, 2014, vol. 260, p. 292. http://dx.doi.org/10.1016/j.jpowsour.2014.02.102
111. Ohta, S., Kobayashi, T., Seki, J., and Asaoka, T., Electrochemical performance of an all-solid-state lithium ion battery with garnet-type oxide electrolyte, *J. Power Sources*, 2012, vol. 202, p. 332. DOI: 10.1016/j.jpowsour.2011.10.064
112. Kotobuki, M., Suzuki, Y., Munakata, H., Kanamura, K., Sato, Y., Yamamoto, K., and Yoshida, T., Fabrication of Three-Dimensional Battery Using Ceramic Electrolyte with Honeycomb Structure by Sol–Gel Process, *J. Electrochem. Soc.*, 2010, vol. 157, p. A493. DOI: 10.1149/1.3308459
113. Li, C., Zhang, B., and Fu, Z., Physical and electrochemical characterization of amorphous lithium lanthanum titanate solid electrolyte thin-film fabricated by e-beam evaporation, *Thin Solid Films*, 2006, vol. 515, p. 1886. DOI: 10.1016/j.tsf.2006.07.026
114. Kotobuki, M., Suzuki, Y., Munakata, H., Kanamura, K., Sato, Y., Yamamoto, K., and Yoshida, T., Compatibility of $LiCoO_2$ and $LiMn_2O_4$ cathode materials for $Li_{0.55}La_{0.35}TiO_3$ electrolyte to fabricate all-solid-state lithium battery, *J. Power Sources*, 2010, vol. 195, p. 5784. DOI: 10.1016/j.jpowsour.2010.03.004
115. Visbal, H., Aihara, Y., Ito, S., Watanabe, T., Park, Y., and Doo, S., The effect of diamond-like carbon coating on $LiNi_{0.8}Co_{0.15}Al_{0.05}O_2$ particles for all solid-state lithium-ion batteries based on $Li_2SeP_2S_5$ glass-ceramics, *J. Power Sources*, 2016, vol. 314, p. 85. http://dx.doi.org/10.1016/j.jpowsour.2016.02.088
116. Seino, Y., Ota, T., and Takada, K., High rate capabilities of all-solid-state lithium secondary batteries using $Li_4Ti_5O_{12}$-coated $LiNi_{0.8}Co_{0.15}Al_{0.05}O_2$ and a sulfide-based solid electrolyte, *J. Power Sources*, 2011, vol. 196, p. 6488. DOI: 10.1016/j.jpowsour.2011.03.090
117. Sakuda, A., Takeuchi, T., and Kobayashi, H., Electrode morphology in all-solid-state lithium secondary batteries consisting of $LiNi_{1/3}Co_{1/3}Mn_{1/3}O_2$ and Li_2S-P_2S_5 solid electrolytes, *Solid State Ionics*, 2016, vol. 285, p. 112. http://dx.doi.org/10.1016/j.ssi.2015.09.010
118. Kitsche, D., Tang, Y., Ma, Y., Goonetilleke, D., Sann, J., Walther, F., Bianchini, M., Janek, J., and Brezesinski, T., High Performance All-Solid-State Batteries with a Ni-Rich NCM Cathode Coated by Atomic Layer Deposition and Lithium Thiophosphate Solid Electrolyte, *ACS Appl. Energy Mater.*, 2021, vol. 4, p. 7338. https://doi.org/10.1021/acsaem.1c01487
119. Ding, J., Sun, Q., and Fu, Z., Layered $Li(Ni_{1/4}Co_{1/2}Mn_{1/3})\ O_2$ as Cathode Material for All-Solid-State Thin-Film Rechargeable Lithium-Ion Batteries, *Electrochem. Solid State Lett.*, 2010, vol. 13, p. A105. DOI: 10.1149/1.3432254
120. Neudecker, B.J., Zuhr, R.A., Robertson, J.D., and Bates, J.B., Lithium Manganese Nickel Oxides $Li_x(Mn_yNi_{1-y})_{2-x}O_2$. II. Electrochemical Studies on Thin-Film Batteries, *J. Electrochem. Soc.*, 1998, vol. 145, p. 4160. DOI: 10.1149/1.1838930

121. Hoshina, K., Yoshima, K., Kotobuki, M., and Kanamura, K., Fabrication of $LiNi_{0.5}Mn_{1.5}O_4$ thin film cathode by PVP sol–gel process and its application of all-solid-state lithium ion batteries using $Li_{1+x}Al_xTi_{2-x}(PO_4)_3$ solid electrolyte, *Solid State Ionics*, 2012, vol. 209–210, p. 30. DOI: 10.1016/j.ssi.2011.12.018

122. Lethien, C., Zegaoui, M., Roussel, P., Tilmant, P., Rolland, N., and Rolland, P.A., Micro-patterning of LiPON and lithium iron phosphate material deposited onto silicon nanopillars array for lithium ion solid state 3D micro-battery, *Microelectron. Eng.*, 2011, vol. 88, p. 3172. DOI: 10.1016/j.mee.2011.06.022

123. Dobbelaere, T., Mattelaer, F., Dendooven, J., Vereecken, P., and Detavernier, C., Plasma-Enhanced Atomic Layer Deposition of Iron Phosphate as a Positive Electrode for 3D Lithium-Ion Microbatteries, *Chem. Mater.*, 2016, vol. 28, p. 3435. DOI: 10.1021/acs.chemmater.6b00853

124. Aboulaich, A., Bouchet, R., Delaizir, G., Seznec, V., Tortet, L., Morcrette, M., Rozier, P., Tarascon, J.-M., Viallet, V., and Dollé, D., A New Approach to Develop Safe All-Inorganic Monolithic Li-Ion Batteries, *Adv. Energy Mater.*, 2011, vol. 1, p. 179. DOI: 10.1002/aenm.201000050

125. Kobayashi, E., Plashnitsa, L.S., Doi, T., Okada, S., and Yamaki, J., Electrochemical properties of Li symmetric solid-state cell with NASICON-type solid electrolyte and electrodes, *Electrochem. Commun.*, 2010, vol. 12, p. 894. DOI: 10.1016/j.elecom.2010.04.014

126. Huang, F., Fu, Z.W., Chu, Y.Q., Liu, W.Y., and Qin, Q.Z., Characterization of Composite 0.5Ag: V_2O_5 Thin-Film Electrodes for Lithium-Ion Rocking Chair and All-Solid-State Batteries, *Electrochem. Solid State Lett.*, 2004, vol. 7, p. A180. DOI: 10.1149/1.1736591

127. Jeon, E.J., Shin, Y.W., Nam, S.C., Cho, W.I., and Yoon, Y.S., Characterization of All-Solid-State Thin-Film Batteries with V_2O_5 Thin-Film Cathodes Using *Ex Situ* and *In Situ* Processes, *J. Electrochem. Soc.*, 2001, vol. 148, p. A318. DOI: 10.1149/1.1354609

128. Navone, C., Baddour-Hadjean, R., Pereira-Ramos, J.P., and Salot, R., Sputtered Crystalline V_2O_5 Thin Films for All-Solid-State Lithium Micro-batteries, *J. Electrochem. Soc.*, 2009, vol. 156, p. A763. DOI: 10.1149/1.3170922

129. Matsumura, T., Nakano, K., Kanno, R., Hirano, A., Imanishi, N., and Takeda, Y., Nickel sulfides as a cathode for all-solid-state ceramic lithium batteries, *J. Power Sources*, 2007, vol. 174, p. 632. DOI: 10.1016/j.jpowsour.2007.06.168

130. Aso, K., Sakuda, A., Hayashi, A., and Tatsumisago, M., All-Solid-State Lithium Secondary Batteries Using NiS-Carbon Fiber Composite Electrodes Coated with $Li_2S–P_2S_5$ Solid Electrolytes by Pulsed Laser Deposition, *ACS Appl. Mater. Interfaces*, 2013, vol. 5, p. 686. dx.doi.org/10.1021/am302164e

131. Jones, S.D., and Akridge, J.R., Development and performance of a rechargeable thin-film state microbattery, *J. Power Sources*, 1995, vol. 54, p. 63. https://doi.org/10.1016/0378–7753(94)02041-Z

132. Chen, M., Yin, X., Reddy, M.V., and Adams, S., All-solid-state $MoS_2/Li_6PS_5Br/In–Li$ batteries as a novel type of Li/S battery, *J. Mater. Chem. A*, 2015, vol. 3, p. 10698. DOI: 10.1039/c5ta02372f

133. Mauger, A., Julien, C.M., Paolella, A., Armand, M., and Zaghib, K., Building Better Batteries in the Solid State: A Review, *Materials*, 2019, vol. 12, article # 3892. DOI: 10.3390/ma12233892

134. Singer, C., Schnell, J., and Reinhart, G., Scalable Processing Routes for the Production of All-Solid-State Batteries – Modeling Interdependencies of Product and Process, *Energy Technol.*, 2021, vol. 9, article # 2000665. https://doi.org/10.1002/ente.202000665

135. Xiao, Y., Wang, Y., Bo, S., Kim, J.C., Miara, L.J., and Ceder, G., Understanding interface stability in solid-state batteries, *Nat. Rev. Mater.*, 2020, vol. 5, p. 105. https://doi.org/10.1038/s41578–019–0157–5

136. Fan, L., He, H., and Nan, C., Tailoring inorganic–polymer composites for the mass production of solid-state batteries, *Nat. Rev. Mater.*, 2021, vol. 6, p. 1003. https://doi.org/10.1038/s41578–021–00320–0

137. Banerjee, A., Wang, X., Fang, C., Wu, E.A., and Meng, Y.S., Interfaces and Interphases in All-Solid-State Batteries with Inorganic Solid Electrolytes, *Chem. Rev.*, 2020, vol. 120, p. 6878. https://doi.org/10.1021/acs.chemrev.0c00101